# Solute dispersion in channels with periodically varying apertures

Diogo Bolster,[1,a)] Marco Dentz,[1,b)] and Tanguy Le Borgne[2,c)]
[1]*Department of Geotechnical Engineering and Geosciences, Technical University of Catalonia (UPC), Barcelona 08034, Spain*
[2]*Géosciences Rennes, UMR 6118, CNRS, Université de Rennes 1, Rennes 35000, France*

(Received 29 October 2008; accepted 20 April 2009; published online 13 May 2009)

We study solute dispersion in channels with periodically varying apertures. Based on an approximate analytical solution of the flow equation, we study the impact of the geometry and molecular diffusion on effective solute dispersion analytically using the method of local moments. We also study the problem numerically using a random walk particle tracking method. For transport in parallel shear flow, the effective dispersion coefficient is dependant on the square of the Peclet number. Here, when the fluctuation of the channel aperture becomes comparable with the channel width, the effective dispersion coefficients show a more complex dependence on the Peclet number and the pore geometry. We find that for a fixed flow rate, periodic fluctuations of the channel aperture can lead to both a decrease and an increase in effective dispersion. © *2009 American Institute of Physics*. [DOI: 10.1063/1.3131982]

## I. INTRODUCTION

The understanding and quantification of the dispersion of dissolved substances in the flow through channels is of importance in a series of applications ranging from the design of microfluidic devices,[1,2] nutrient transport in blood vessels,[3,4] dispersion in porous media,[5–9] and mixing and spreading of contaminants in groundwater aquifers.[10–13] Groundwater aquifers are frequently modeled as heterogeneous porous media whose pore scale structure can be represented by a network of pore channels.[14] Fractured geological media are often represented as networks of discrete fractures.[15,16] Thus, studying the channel model under consideration here gives valuable insight in the pore scale mixing and spreading processes which are of paramount importance for the correct modeling of mixing-limited reactive transport in porous media, as pointed out, for example, by Ref. 17.

The volume occupied by a solute dissolved in the fluid flow through a channel expands at short time scales due to molecular diffusion. Eventually at some intermediate scale, the interaction of molecular diffusion, local flow variability, and the geometry of the channel leads to a mixing and spreading behavior that is different from the one induced by molecular diffusion. In general, when dealing with solute transport in inhomogeneous environments, one distinguishes between spreading, which consists in increasing the surface area of a solute plume, and mixing and dilution, which consists in increasing the volume occupied by a dissolved substance in the host fluid.[13,18–20] This distinction is of particular importance at preasymptotic times, that is, at times, for which the solute has not sampled the full geometrical and flow variability.[13,20–22] At asymptotic times, solute spreading can be measured by constant dispersion coefficients that integrate the interaction of small scale spatial variability and diffusion on effective spreading and mixing. Many studies[5,23,24] focus on the determination of the coefficient that describe the effective solute dispersion on the large scale, i.e., at length and time scales on which the microscale variability of flow and geometry are homogenized.

The impact of the interaction of molecular diffusion and flow variability on effective solute dispersion in axisymmetric channels was studied by Taylor[23] and Aris.[25] They showed that given enough time for vertical concentration gradients to be smeared out by diffusion, effective solute transport is one dimensional and completely defined by the mean flow velocity $U$ and the effective Taylor dispersion coefficient,[23]

$$D^* = D + \frac{U^2 a^2}{210D}, \tag{1}$$

where $D$ is the molecular diffusion coefficient and $a$ is the channel width. This result relies on a constant channel aperture.

In many applications, however, channel apertures are not constant. The geometry of the channel can have a significant impact on the effective dispersion behavior and lead to a behavior that is qualitatively and quantitatively different from the one found in channels with constant aperture. In microfluidics, for example, the design of specific mixing properties in microchannels is based on the manipulation of the channel geometry.[1] The channel model is also of interest to study solute dispersion in geological media.[26–28] Although natural media is in general not periodic, it represents the simplest system to analyze the effect of the convergence and divergence of flow lines on dispersion. The latter plays a central role for transport in heterogeneous porous media. At fracture scale, the proposed channel model is relevant to understand the role of fracture wall roughness on the transport properties. Tartakovsky and co-worker[29,30] studied the impact of small scale roughness on the global dispersion using

a)Electronic mail: diogo.bolster@gmail.com.
b)Electronic mail: marco.dentz@upc.edu.
c)Electronic mail: tanguy.le-borgne@univ-rennes1.fr.

 

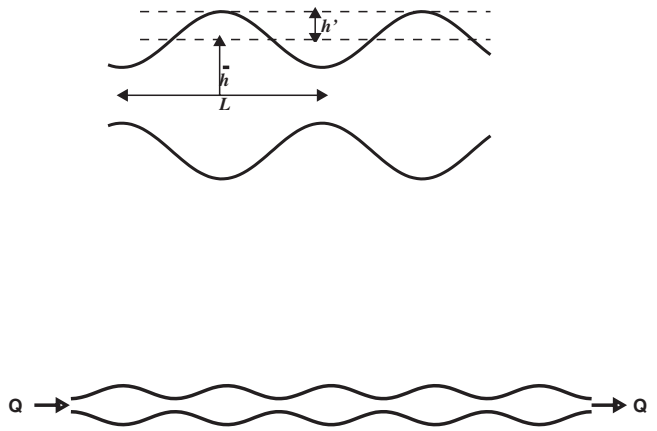


FIG. 1. A schematic of the pore we are considering and a connected periodic network of pores

a stochastic model. Using an alternate stochastic model[31] estimated the dispersion due to fluctuations in the boundary and within this framework always observed an increase in dispersive effects due to fluctuations. Studying transport in self-affine rough fractures, Drazer *et al.*[32,33] illustrated that surface roughness could reduce dispersion effects at very low Peclet numbers. Smith[34] analyzed longitudinal dispersion coefficients for varying channels. Mercer and Roberts[35] investigated effective solute transport in channels with varying flow properties using center manifold theory. Rosecrans[36] studied Taylor dispersion in curved channels using the same approach. In the latter paper a heuristic argument is given for the existence of channel shapes and flow fields that lead to a reduction instead of an increase in solute dispersion as it is observed in channels with constant aperture. Hoagland and Prud'homme[37] studied the transport of a passive solute in a sinusoidal tube in a pressure driven flow. Other authors (e.g., Refs. 38–40) looked at transport by processes such as thermophoresis and electrophoresis (force, rather than pressure driven) in sinusoidal geometries and quantified the dependence of transport properties on Peclet number and geometry.

The geometry of the pore has a significant impact on the flow velocity. Here we focus on flow regimes at small Reynolds numbers so that the flow problem is given by Stokes equation. Kitanidis and Dykaar[12] derived an analytical expression for the velocity distribution in a channel that consists of a connected periodic chain of slowly varying two-dimensional pores, as illustrated in Fig. 1. Their analysis demonstrates that short wavelengths and large amplitudes can give rise to recirculation zones. Such recirculation zones represent immobile regions that can have a significant impact on effective solute transport depending on the typical mass transfer time scales.[41–45] Similar results for the flow velocity in periodic channels were obtained in Refs. 46–48. Specifically Cao and Kitanidis[47] illustrated the existence of recirculation zones for pores that open rapidly.

The methods devised by Taylor and Aris for the calculation of asymptotic dispersion coefficients are typically restricted to parallel flows. In a series of seminal papers a "generalized" theory of dispersion was developed for passive[5,49,50] as well as reactive flows.[51,52] These methods allow for the calculation of the asymptotic effective dispersion and reaction coefficients for flow domains having a periodic structure.

Based on this generalized theory of dispersion, Dykaar and Kitanidis[53] studied macrotransport of a reactive solute in a porous medium on the basis of the analytical expression for the pore velocity field given in Ref. 12. They determined the combined effects of reaction, flow variability. and molecular diffusion on macrotransport for a particular pore geometry which included a recirculation zone.

In this paper, we systematically study the impact of pore scale geometry and molecular diffusion on asymptotic solute dispersion using the analytical expression for the flow velocity given in Ref. 12. We investigate analytically and numerically under which conditions solute dispersion can decrease and probe the impact of recirculation zones on asymptotic dispersion. To this end, we apply the approach by Taylor[23] and Aris[25] as well as the one devised by Brenner[5] to determine the asymptotic longitudinal dispersion coefficient and compare them to the dispersion coefficients obtained by numerical random walk simulations.

## II. PORE GEOMETRY AND FLOW VELOCITY

We consider flow in a channel that is two dimensional and symmetric about a central axis at $y=0$. The channel walls fluctuate periodically in horizontal direction,

$$h(x) = \bar{h} + h' \sin\left(\frac{2\pi x}{L}\right), \tag{2}$$

where $\bar{h}$ is the average channel height and $h'$ is the amplitude of the fluctuations. A unit cell in the following is denoted by $\Omega$, its volume by $V_\Omega$. The aspect ratio is defined by

$$\epsilon = \frac{2\bar{h}}{L}. \tag{3}$$

The ratio between the amplitude of the aperture fluctuations $h'$ and the mean aperture in the following called the fluctuation ratio, is denoted by

$$a = \frac{h'}{2\bar{h}}. \tag{4}$$

The flow rate through the channel $Q$ and the fluid viscosity $\nu$ define the Reynolds numbers

$$\mathrm{Re} = \frac{Q}{\nu}. \tag{5}$$

On the pore scale, Reynolds numbers are typically small[12,14] of the order of $10^{-4}$–$10^{-1}$. For Reynolds number of this scale flow is described by the Stokes equation.

For a slowly varying boundary, i.e., $\epsilon \ll 1$ Kitanidis and Dykaar[12] derived an analytical solution for the flow velocity using a perturbation expansion in $\epsilon$. In the following, we give a brief summary of their solution. For a detailed derivation we refer the reader.[12]

The divergence-free flow velocity $\mathbf{u}=(u,v)^T$ is given in terms of the stream function $\Psi$ by

$$u = \frac{\partial \Psi}{\partial y}, \quad v = -\frac{\partial \Psi}{\partial x}. \tag{6}$$

The flow equation for $\Psi$ is biharmonic,[12,54]

$$\nabla^4 \Psi = 0. \tag{7}$$

At the channel walls no-flux and no-slip boundary conditions are specified. The solution for $\Psi$ is periodic with period $L$. In addition to mass and momentum balance as expressed by Eq. (7) the solution of the flow problem requires a further equation expressing energy conservation.[12] The viscous dissipation energy within a cell of length $L$ is balanced by the work applied to the fluid in the cell volume,[12,55]

$$\int_\Omega \mathrm{d}V \nu \Theta = -\Delta p Q, \tag{8}$$

where $\Theta$ is the dissipation function,[55] $\Delta p$ is the pressure drop over the unit cell, and $Q$ is the flow rate.

Note that the flow rate in a channel with constant aperture given by the average aperture $2\bar{h}$ is described by the cubic law,[14,56]

$$\bar{Q} = -\frac{2\bar{h}^3}{3\nu}\frac{\Delta p}{L}. \tag{9}$$

For the case of sinusoidally varying walls, however, it is known that the cubic law does not hold.[48]

Kitandis and Dykaar[12] performed a perturbation expansion of the stream function $\psi$ and the flow rate $Q$ in powers of $\epsilon$,

$$\Psi = \sum_{i=0}^{\infty} \epsilon^i \Psi_i, \quad Q = \sum_{i=0}^{\infty} \epsilon^i Q_i. \tag{10}$$

They determine the contributions up to fourth order, where $\Psi_1=\Psi_3=0$ and $Q_1=Q_3=0$. Their explicit results for $\Psi_0$, $\Psi_2$, and $\Psi_4$, and $Q_0$, $Q_2$, and $Q_4$ are given in Appendix A for completeness. Accordingly, we obtain for the flow velocity,

$$\mathbf{u}(\mathbf{x}) = \sum_{i=0}^{\infty} \epsilon^i \mathbf{u}^{(i)}(\mathbf{x}). \tag{11}$$

In order to illustrate the different types of flow that can arise within such a geometry, three sets of streamlines calculated using Eq. (10) are shown in Fig. 2. Figure 2(a) shows the channel flow for $\epsilon=0$. It is given by the well known Hagen–Poiseuille flow. For increasing $\epsilon$, the streamlines become more curved, see Fig. 2(a) for $\epsilon=0.2$. For $\epsilon=0.4$, Fig. 2(c), recirculation cells develop at the location of the maximum channel diameter.

The deviation of the flux $Q$ from the cubic law is illustrated in Fig. 3 for the contributions $Q_0$, $Q_2$, and $Q_4$ normalized by $\bar{Q}$, Eq. (9), which follows the cubic law. Figure 3 illustrates how the three quantities vary with varying fluctuation ratio $a$. The pressure drop $\Delta P$ across each pore is identical. $Q_0$ decreases monotonically with $a$, which is a reflection on the fact that a given pressure drop will cause less flow for highly fluctuating pores, eventually approaching zero as the thinnest section of the pore approaches zero too ($h' \to h$, i.e., if there is zero cross sectional area no matter how large the pressure drop no flow can occur).

$Q_2$ is a negative quantity, which is zero for $h'=0$ and $h'=h$. This suggests that second-order effects can cause a reduction in effective flow rate and thus perhaps also dispersion. Finally $Q_4$ is always positive with zero value at $h'=0$ and $h'=h$.

## III. SOLUTE DISPERSION

Transport in the flow field through a two-dimensional channel with varying diameter is described by the advection diffusion equation. The temporal change in the solute distribution $c(\mathbf{x},t)$ is balanced by the divergence of the advective-diffusive solute flux

$$\frac{\partial c(\mathbf{x},t)}{\partial t} + \nabla \cdot [\mathbf{u}(\mathbf{x}) - D\nabla] c(\mathbf{x},t) = 0, \tag{12}$$

where $D$ is the molecular diffusion coefficient. We investigate the asymptotic longitudinal dispersion behavior of a dissolved substance. The boundary conditions are natural boundary conditions at $x=\pm\infty$ and vanishing solute flux at the periodically fluctuating horizontal boundary. The initial distribution is given by $c(\mathbf{x},t=0)=\rho(y)\delta(x)$, i.e., a vertical line source.

The longitudinal flow velocity $u(\mathbf{x})$ is divided into its average value over the unit cell

$$\bar{u} = \frac{D}{V_\Omega}\int_\Omega d\mathbf{x} u(\mathbf{x}), \tag{13}$$

and fluctuations about it,

$$u(\mathbf{x}) = \bar{u}[1 + u'(\mathbf{x})]. \tag{14}$$

Flow and transport can be characterized by two dimensionless numbers; the aspect ratio $\epsilon$, Eq. (3), and the Peclet number Pe, which is defined by

$$\mathrm{Pe} = \frac{2\bar{h}\bar{u}}{D}. \tag{15}$$

The Peclet number denotes the ratio between the advective and dispersive time scales

$$\tau_u = \frac{2\bar{h}}{\bar{u}}, \quad \tau_D = \frac{(2\bar{h})^2}{D}, \tag{16}$$

respectively.

Solute dispersion here is characterized in terms of the longitudinal width $\kappa$ of the solute distribution $c(\mathbf{x},t)$,

$$\kappa(t) = \int d\mathbf{x} x^2 c(\mathbf{x},t) - \left[\int d\mathbf{x} x c(\mathbf{x},t)\right]^2. \tag{17}$$

Specifically, asymptotic longitudinal dispersion is quantified in terms of the effective dispersion coefficient

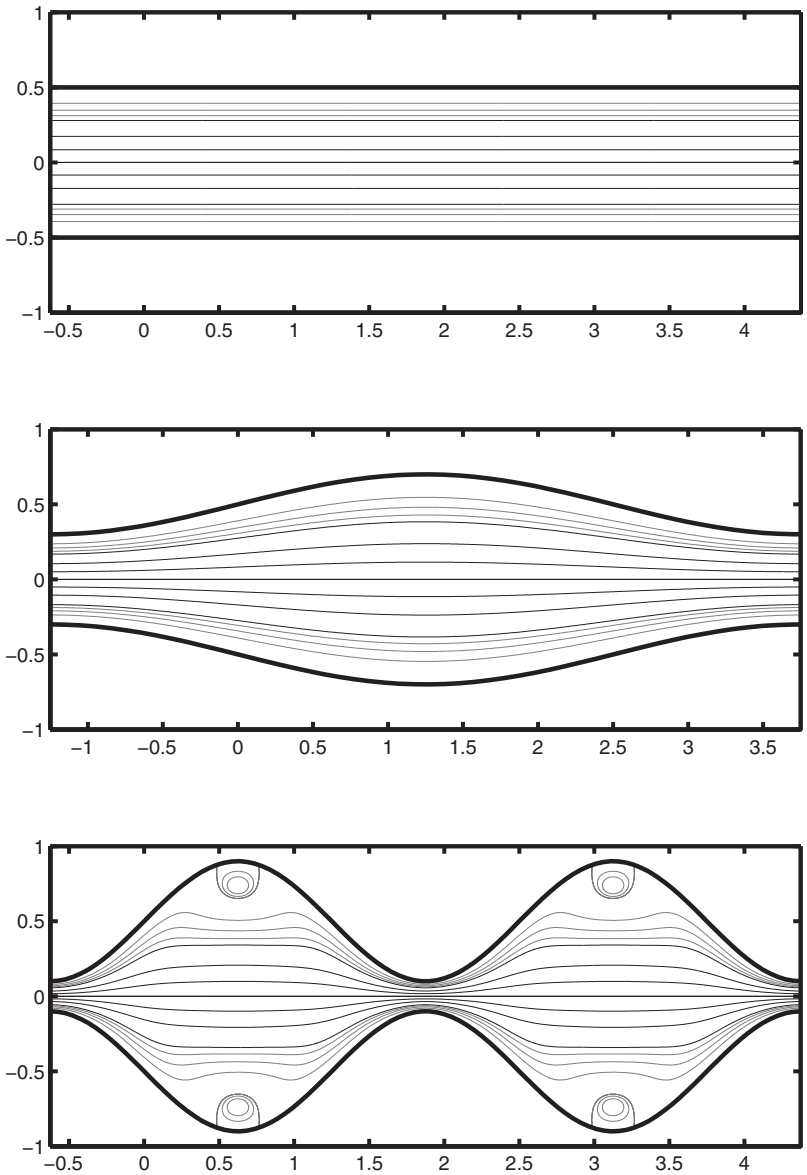

FIG. 2. Streamlines for a pore with $\epsilon=0$ and $a=0$ (top), $\epsilon=0.2$ and $a=0.2$ (middle), and $\epsilon=0.4$ and $a=0.4$ (bottom).

$$D^e = \frac{1}{2}\lim_{t\to\infty}\frac{d\kappa(t)}{dt}. \tag{18}$$

Brenner[5] determined the following expression for the dispersion coefficient in periodic flow scenarios, using the method of local moments:

$$D^e = \frac{D}{V_\Omega}\int_\Omega d\mathbf{x}\left[\nabla\chi(\mathbf{x})\cdot\nabla\chi(\mathbf{x}) + 2\frac{\partial\chi(\mathbf{x})}{\partial x}\right], \tag{19}$$

where the auxiliary function $\chi(\mathbf{x})$ satisfies

$$-D\nabla^2\chi(\mathbf{x}) + \nabla\cdot\mathbf{u}(\mathbf{x})\chi(\mathbf{x}) = -u'(\mathbf{x}). \tag{20}$$

The boundary conditions for $\chi(\mathbf{x})$ are

$$\nabla\cdot\mathbf{u}(\mathbf{x})\chi(\mathbf{x}) = 0 \tag{21}$$

for $\mathbf{x}\in\partial\Omega$, where $\partial\Omega$ is the boundary of the unit cell. Furthermore, $\chi$ is periodic and its integral over the unit cell is zero

$$\int_\Omega d\mathbf{x}\chi(\mathbf{x}) = 0. \tag{22}$$

Using these properties of $\chi(\mathbf{x})$ it is easy to show by applying the Gauss theorem that Eq. (19) can be written as

$$D^e = \frac{1}{V_\Omega}\int_\Omega d\mathbf{x}\left[-u'(\mathbf{x})\chi(\mathbf{x}) + 2D\frac{\partial\chi(\mathbf{x})}{\partial x}\right]. \tag{23}$$

In order to solve for the asymptotic dispersion tensor, we first employ an approximation in the spirit of Taylor's derivation[23] of an effective dispersion coefficient in parallel channels, second we numerically solve Eqs. (19) and (20) and third, we use numerical random walk simulations to solve the full transport problem. The results are compared against the numerical simulations.

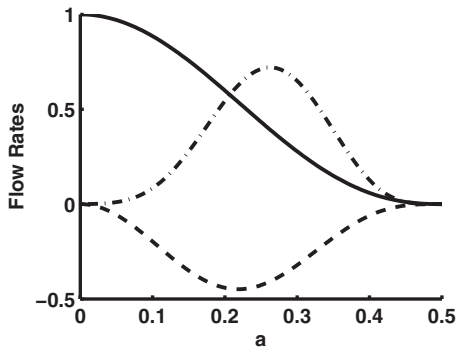


FIG. 3. Normalized $Q_0$ (–), $Q_2$ (- -), and $Q_4$ (-.) as a function of the fluctuation ratio $a$.

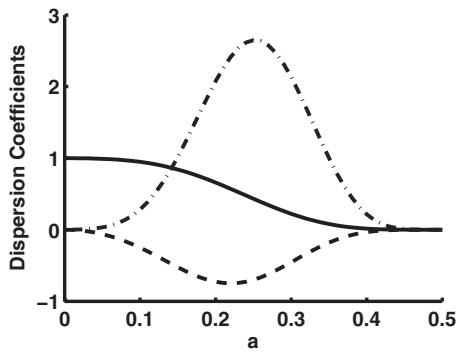


FIG. 4. Dispersion coefficients as a function of $a$. $D_0^e$ (–), $D_2^e$ (- -), and $D_4^e$ (-.).

### A. Taylor approximation

We assume that vertical gradients of $\chi(\mathbf{x})$ are much larger than longitudinal ones. We furthermore assume that advective transport vertical to the channel axis can be disregarded. Thus, Eq. (20) simplifies to

$$-D\frac{\partial^2\chi(\mathbf{x})}{\partial y^2}=-u'(\mathbf{x}). \tag{24}$$

This approximation is motivated by the original assumptions made by Taylor[23] and Aris[25] and a desire to know how far they can take use. It is similar to the Fick–Jacobs approximation in thermophoretic transport.[40] As shown by Yariv and Dorman (2007),[38] the approximation becomes invalid when Pe $\epsilon^2\sim O(1)$, where the other terms in Eq. (20) make a more significant contribution. Nonetheless it is important to study it to see how far such an approximation can take you and what type of error one may expect if it is made as it plays an important role in the validity of the cubic law and its Taylor dispersion interpretation.[31,57,14,56] Equation (24) can be integrated straightforwardly as outlined in Appendix B. Note that the present approximation requires the disregard of horizontal gradients of $\chi(\mathbf{x})$ in expression (19) for the effective asymptotic dispersion coefficient, which is equivalent to directly employing Eq. (23).

#### 1. Effective dispersion coefficient

Using expansion (11) for the flow velocity, we obtain an expansion in $\epsilon$ for $\chi$

$$\chi(\mathbf{x})=\sum_{i=0}^{\infty}\epsilon^i\chi_i(\mathbf{x}). \tag{25}$$

Inserting the latter into Eq. (19) yields for the effective dispersion coefficient,

$$D^e=\sum_{i=0}^{\infty}\epsilon^i D_i^e, \tag{26a}$$

$$D_i^e=\sum_{j=0}^{i}\frac{D}{V_\Omega}\int_\Omega d\mathbf{x}\frac{\partial\chi^{(i-j)}(\mathbf{x})}{\partial y}\frac{\partial\chi^{(j)}(\mathbf{x})}{\partial y}+\frac{2D}{V_\Omega}\int_\Omega d\mathbf{x}\frac{\partial\chi^{(i)}(\mathbf{x})}{\partial x}. \tag{26b}$$

Solving Eq. (24) and using Eq. (6) we obtain for the zeroth order contribution to $D^e$,

$$D_0^e=\frac{1}{210}\frac{Q_0^2}{D}+\frac{a^2}{10}\frac{Q_0^2}{D}. \tag{27}$$

Note that this term consists of one part that is analog to the classic Taylor dispersion result with the difference that $Q_0$ does not follow the cubic law and a second term that depends on the fluctuation size $a$. One might expect this zero-order analysis to hold for any flow where the boundary fluctuates slowly over a length scale larger than the average channel width as this corresponds to a lubrication theory type approach.[58]

The second-order contribution to the effective dispersion coefficient is given by

$$D_2^e=\frac{1}{D}\left[\frac{1}{5}a^2Q_0^2+\frac{1}{105}Q_0Q_2-\frac{2}{25}a^4\pi^2Q_0^2+\frac{2}{175}a^2\pi^2Q_0^2\right]. \tag{28}$$

Similarly at fourth order, we obtain

$$D_4^e=\frac{1}{D}\left(\frac{71}{606\,375}a^2\pi^4Q_0^2+\frac{2918}{40\,425}a^4\pi^4Q_0^2-\frac{548\,381}{4\,036\,032\,000}Q_0^2a^2\pi^6-\frac{2}{875}Q_0^2a^6\pi^4+\frac{4}{175}Q_0Q_2a^2\pi^2-\frac{4}{25}Q_0Q_2a^4\pi^2+\frac{1}{5}Q_0Q_4a^2+\frac{1}{10}Q_2^2a^2+\frac{1}{210}Q_2^2+\frac{1}{105}Q_0Q_4\right). \tag{29}$$

Using the flow rates given in Appendix A we can compute the contributions to the effective dispersion coefficients from Eqs. (27)–(29). The dependence of $D^e$ on $a$ is illustrated Fig. 4. Note here that the decrease in $D_0^e$ with $a$ is not

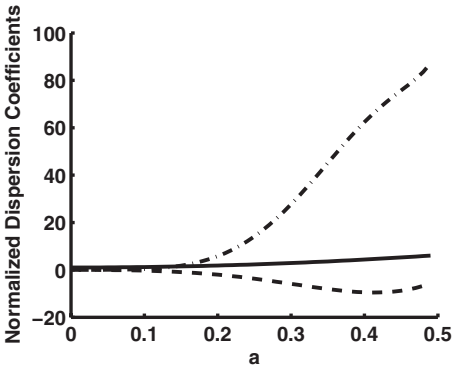


FIG. 5. $\mathcal{D}_{e0}$ (–), $\mathcal{D}_{e2}$ (- -), and $\mathcal{D}_{e4}$ (-.) for various values of $a$.

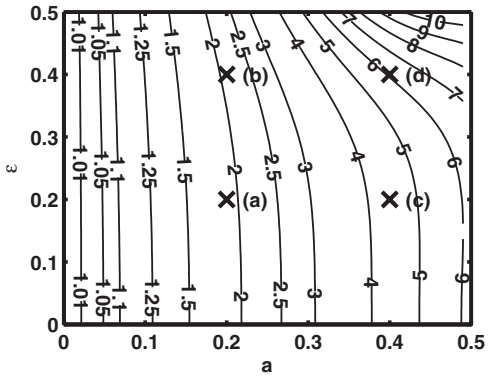


FIG. 6. Contour plot of normalized $\mathcal{D}_{e0}+\epsilon^2\mathcal{D}_{e2}+\epsilon^4\mathcal{D}_{e4}$ over various values of a and $\epsilon$. The four points marked with an × correspond to the four points we will focus our attention on in numerical simulations. They correspond to (a) $\epsilon=0.2$ and $a=0.2$, (b) $\epsilon=0.4$ and $a=0.2$, (c) $\epsilon=0.2$ and $a=0.4$, and (d) $\epsilon=0.4$ and $a=0.4$.

due to pore geometry but reflects the fact that the flow rate $Q_0$ decreases with increasing $a$ for a constant pressure drop. Note that $D_0^e$ decreases more rapidly with $a$ than $Q_0$ did because of the quadratic relationship. It is worth noting that $D_2^e$ is negative, reflecting the influence of $Q_2$.

### 2. Dependence on the pore wall geometry

From Fig. 4 we have seen that due to nonlinear effects through the orders $D^e$ does not scale with $Q$ in the same manner as for transport in a parallel channel flow. In order to study the dependence of the dispersion properties on the pore wall geometry, we choose the flow rate $Q_{\text{tot}}=Q_0+\epsilon^2Q_2+\epsilon^4Q_4$ such that the average flow rate is always the same regardless of $a$ and $\epsilon$ (i.e., we no longer impose a fixed pressure drop, but rather a constant flow rate). Additionally, in order to compare the relative impact or the curvature, we normalize all dispersion coefficients by the dispersion coefficient for normal parallel flow, i.e.,

$$\mathcal{D}^e = \frac{D^e}{D^e|_{a=0,\epsilon=0}}. \tag{30}$$

$\mathcal{D}^e$ is a dimensionless dispersion coefficient. As the values of Eqs. (27)–(29) are difficult to interpret intuitively due to the size and complexity of the expressions, a plot illustrating the values of $\mathcal{D}_0^e$, $\mathcal{D}_2^e$, and $\mathcal{D}_4^e$ for several values of $a$ is shown in Fig. 5. One feature in this figure that should raise caution is the relatively large values of $\mathcal{D}_4^e$ compared to $\mathcal{D}_0^e$ for larger values of $a$. This suggests that for these larger values of $a$ the asymptotic expansion in Eq. (25) may become invalid and that as such one must be cautious in interpreting these results. As $\mathcal{D}_4^e$ is multiplied by $\epsilon^4$ these contributions can still be relatively small.

A contour plot showing $\mathcal{D}^e$ for various values of $a$ and $\epsilon$ is shown in Fig. 6. Now that the effect of decreased flow rate due to a constant pressure drop has been removed it is evident that the boundary fluctuations could potentially have significant influence on the overall enhanced Taylor dispersion, particularly for large values of $a$ and $\epsilon$, which corresponds to shorter pores with large boundary fluctuations.

In order to investigate this further we will focus on four points illustrated in Fig. 6 marked (a)–(d). Using this classical model we would expect an increase in Taylor dispersion by a factor of (a) 1.87, (b) 2.06, (c) 4.4, and (d) 5.93. The only one of these cases that has a recirculation zone is case (d).

Figure 7 depicts a surface plot of the total dispersion coefficient, normalized by the parallel wall case, over a range $0<a<0.45$ and $0.01<\epsilon<0.5$ for various typical Peclet numbers. It is worth noting that the behavior for all cases is similar with any increase in $\epsilon$ or $a$ resulting in an increase in the effective dispersion coefficient. Once the Peclet number is large the relative changes in behavior become identical as seen for the Pe=100, Pe=1000, and Pe=2000 cases. This is simply because for these cases the enhanced dispersion effect is much larger than the molecular diffusion contribution, which still plays a significant enough role for the Pe=10 case.

## B. Brenner solution

One of the major drawbacks of a straightforward application of the Taylor–Aris predictions for dispersion is the fact that it disregards horizontal gradients and advective mass transfer perpendicular to the mean flow direction. This type of approximation is not valid for larger values of $a$ and $\epsilon$ as the curvature of the flow increases and particularly in the regimes for which recirculation zones appear. In this case we rely on the numerical solution of Eq. (20) for the auxiliary function $\chi(\mathbf{x})$ and Eq. (19) for the asymptotic dispersion coefficient. We employ the finite difference methods outlined in Ref. 53.

Figure 8 illustrates the normalized dispersion coefficient for various values of Peclet number. There are several interesting and perhaps unexpected features illustrated here, particularly in light of what we saw in the previous section and Fig. 7. First, note that the general behavior for each order of Peclet number is different. That is, the figure for Pe=10 is distinct from the one illustrating Pe=100, which in turn is different from the Pe=1000 case. With the result obtained by the Taylor–Aris approximation presented in Sec. III A one

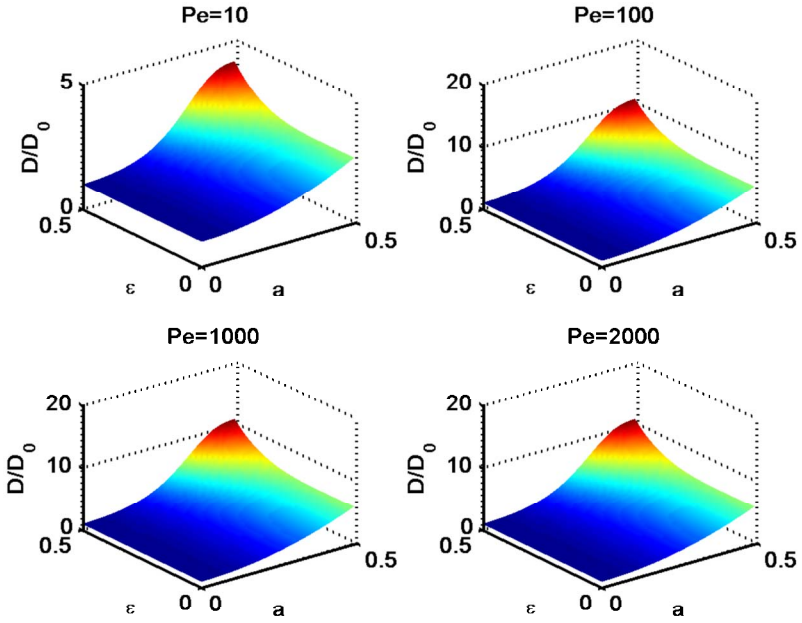


FIG. 7. (Color online) Normalized dispersion coefficients for various values of Peclet number, calculated using the Taylor–Aris approximation model [Eq. (26a)].

would not expect this as the effective dispersion is dependant on the square of the Peclet number (i.e., $D^e \sim D\ \mathrm{Pe}^2$).

Based on simple scaling arguments one might expect an effective dispersion $D^e = \alpha D\ \mathrm{Pe}^2$, where $\alpha$ is a constant that would depends on the geometry, namely, $\epsilon$ and $a$. The results in Fig. 8 seem to indicate that this scaling is not accurate when fluctuations in the pore wall exist.

In particular, the Taylor–Aris results predict that the only effect the fluctuations of the boundaries can have is to increase the effective dispersion. This certainly seems to hold true for the Pe=10 case, although the behavior is not monotonic in $\epsilon$ for all values of $a$. For the larger Peclet number cases, Pe=100, Pe=1000, and Pe=2000, we actually predict that in certain cases the boundary fluctuations decrease the effective dispersion coefficient, particularly for small values of $\epsilon$. Values of the maximum and minimum dispersion coefficients and the respective values of $a$ and $\epsilon$ for each of the Peclet numbers considered are shown in Table I. A cross section of Figs. 7 and 8 at Pe=1000 for $\epsilon$=0.2 is shown in Fig. 9 to illustrate and compare this effect. Note that while the "Taylor–Aris–type" solution increases with $a$, the full solution actually decreases, although the relative magnitude of this change is much less.

Also, in general, one might expect the influence of the boundaries to play a larger role for the larger Peclet number cases, as dispersion is an advectively driven phenomenon

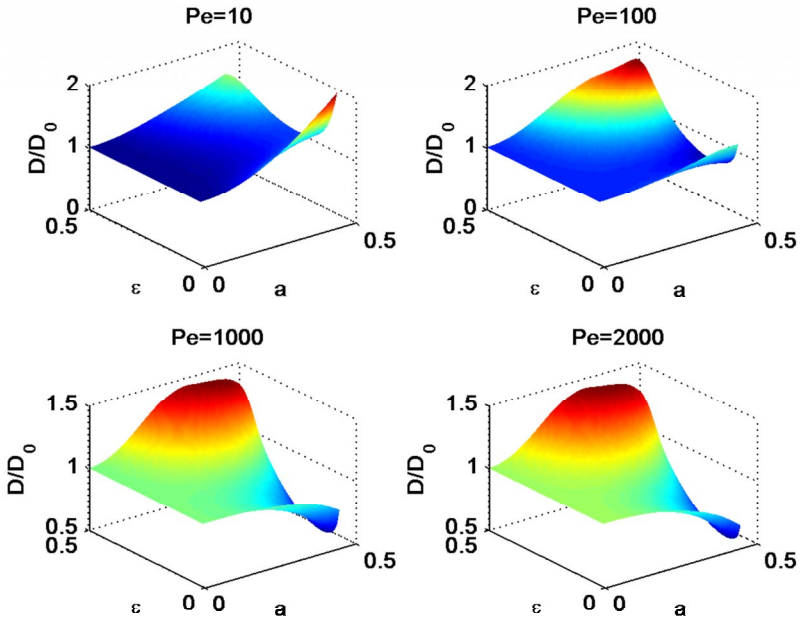


FIG. 8. (Color online) Surface contour plots for the dispersion coefficients for various Peclet numbers over a range of $a$ and $\epsilon$ calculated using Brenner's method [Eq. (23)]. All values are normalized with the value corresponding to a smooth channel (i.e., $a$=0).

TABLE I. Values and locations of the maximum and minimum normalized dispersion coefficients from each of the cases depicted in Fig. 7.

| Pe | Maximum | Location | Minimum | Location |
|---|---|---|---|---|
| 10 | 2.1 | $\epsilon=0.02$ $a=0.45$ | 1 | $\epsilon=0$ $a=0$ |
| 100 | 1.867 | $\epsilon=0.45$ $a=0.45$ | 0.85 | $\epsilon=0.13$ $a=0.45$ |
| 1000 | 1.46 | $\epsilon=0.46$ $a=0.08$ | 0.54 | $\epsilon=0.45$ $a=0.4$ |
| 2000 | 1.46 | $\epsilon=0.46$ $a=0.08$ | 0.52 | $\epsilon=0.45$ $a=0.4$ |

(although diffusion is necessary to activate it). However, the largest relative change in dispersion for these cases seems to occur for Pe=10 for small values of $\epsilon$ and larger $a$. This suggests that for lower Peclet numbers long wavelengths with large amplitudes can increase dispersion. A tentative explanation for these observations is given in Sec. III C.

### C. Random walk simulations

While experiments for the types of flows presented here do exist, changing the geometry and accurate measurements can be elusive. Random walk particle tracking provides an efficient way to determine effective dispersion coefficients.[13,59–63] The random walk simulations presented in the following are based on the Langevin equation

$$\frac{dx(t|\mathbf{x}')}{dt} = u[\mathbf{x}(t|\mathbf{x}')] + \xi_1(t),$$
$$\frac{dy(t|\mathbf{x}')}{dt} = v[\mathbf{x}(t|\mathbf{x}')] + \xi_2(t), \tag{31}$$

where $\mathbf{x}(t|\mathbf{x}')$ denotes the tracetory of a solute particle that is initially located at $\mathbf{x}(t=0|\mathbf{x}')=\mathbf{x}'$. The initial position of a solute particle is denoted by $\mathbf{x}(t=0)=\mathbf{x}'$, which for a line source at $x=0$ is $\mathbf{x}'=(0,b)^t$, where $b$ is uniformly distributed over the channel cross section at $x=0$. The transport description in terms of the Langevin Eq. (31) is exactly equivalent to the one in terms of the Fokker–Planck Eq. (12).[64]

The $\boldsymbol{\xi}(t)$ denotes a two-dimensional Gaussian white noise, which is defined by its first and second moments

$$\langle \xi_i(t) \rangle = 0, \quad \langle \xi_i(t)\xi_j(t') \rangle = 2D\delta_{ij}\delta(t-t'). \tag{32}$$

The numerical solution of Eq. (31) and the calculation of the effective dispersion coefficient (18) using random walk particle tracking are outline in Appendix C.

Figure 10 shows particle distributions at a transport time of $50\tau_u$ for three different Peclet numbers of (a) $\mathrm{Pe}=10^3$, (b) $10^2$, and (c) 10 and the fluctuation ratios $a=0,0.2,0.4$ and apertures of $\epsilon=0.2$ and 0.4.

Note that for the classical Taylor problem ($a=0$), the asymptotic regime is reached at times larger than the diffusion time scale, $t \gg \tau_D$, i.e., when vertical gradients have disappeared due to mixing. For $\mathrm{Pe}=10^3$ and $\mathrm{Pe}=10^2$, the displayed transport time is smaller than $\tau_D$ and the observed distributions are preasymptotic. Nonetheless, these figures illustrate the influence of the boundaries on the dispersion behavior.

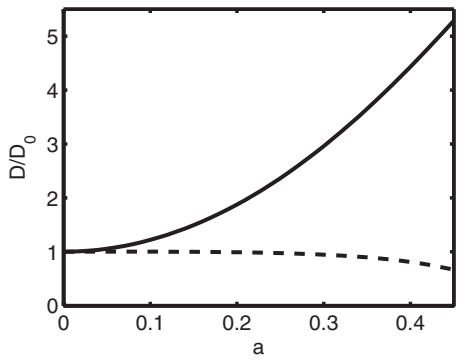


FIG. 9. Normalized dispersion coefficients against $a$ using the Taylor–Aris approximation [Eq. (26a)] (–) and full solution [Eq. (23)] (- -) at Pe=1000 for $\epsilon=0.2$.

Recall Fig. 2, which illustrates the streamlines of the flow field for different values of the aspect ratio $\epsilon$. For $\epsilon=0.4$ a recirculation zone forms where the channel width is maximum. This notes both in the center of mass velocity of the plume as well as in the width compared to the flow fields with the flow fields for smaller aspect ratios. With increasing Peclet number the plume width increases significantly due to a higher residence time of trapped particles in the recirculation zones.

Figure 11 compares the predicted dispersion coefficients for points (a)–(d) from Fig. 7(b) using the parallel wall Taylor solution [i.e., $a=0$, Eq. (1)], our approximate "Taylor–Aris" solution [Eq. (26a)], the Brenner solution [Eq. (23)] and the solutions calculated from the random walk simulations. Even for case (a) the agreement for all cases is not good as the Taylor–Aris approximation overpredicts the effective dispersion coefficient. However, the parallel wall case with no fluctuations seems to work quite well. In cases (b) and (d) the parallel wall solution underpredicts the measured, while the full higher order solution overpredicts it. For case (c), where the influence of the boundaries is to decrease the dispersion, both the parallel wall and full Taylor–Aris predictions are unable to capture this decrease. This clearly illustrates the limitations of a traditional Taylor–Aris approach, which cannot capture the influence of nonparallel flow. This disagreement, particularly evident at larger Pe is unsurprising as the approximation in Eq. (24) becomes invalid when $\mathrm{Pe}\,\epsilon^2=O(1)$ as shown by Ref. 38. Additionally, the asymptotic expansion in Eq. (25) also becomes questionable for the larger values of $a$. On the other hand, the Brenner theory, which does not suffer from this limitation agrees excellently with all the cases presented in Fig. 11.

While the four cases illustrated here seem to indicate that Brenner's theory works at predicting the influence of the boundaries on dispersion we investigated this further by considering the maximum and minimum predicted values for the Pe=10, Pe=100, and Pe=1000 as depicted in Fig. 8. In all cases good agreement was found between Brenner's theory and the random walk simulations, suggesting further that the theory works well.

The results of this study can be understood in a Lagrangian framework. Pore wall fluctuations affect the distribution of Lagrangian velocities within a single pore and the corre-

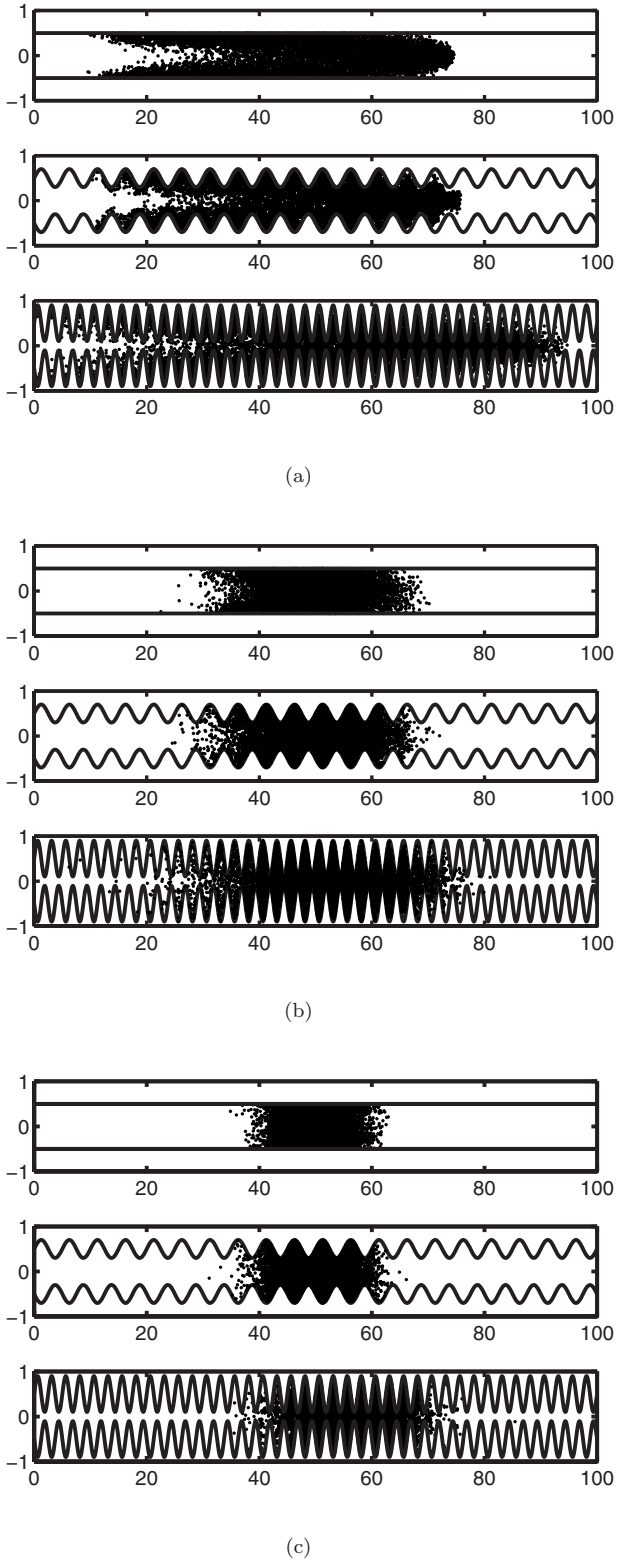


FIG. 10. Random walk simulations at several Peclet numbers after a time of 50T (where 1 T is the advective time scale). In all cases the top plot corresponds to $a=0$, the middle plot to $a=0.2$ and $\epsilon=0.2$, and the bottom plot to $a=0.4$ and $\epsilon=0.4$. (a) Pe=1000, (b) Pe=100, and (c) Pe=10.

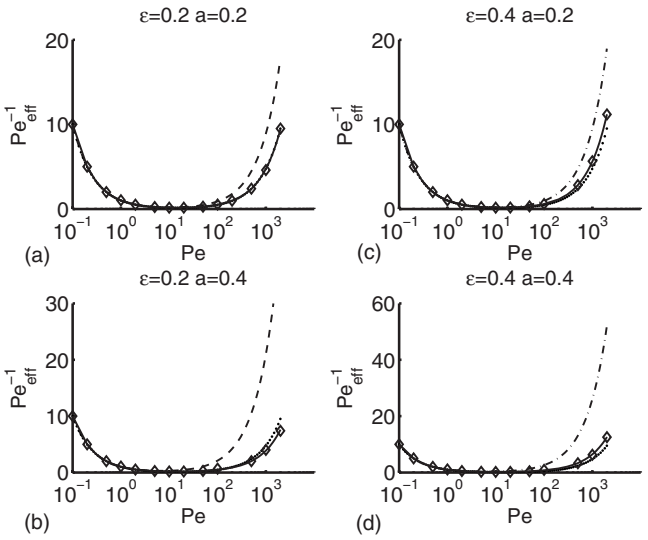


FIG. 11. Taylor dispersion (inverse effective Peclet number) predicted by the Taylor theory, Brenner, and measured by random walks for cases (a)–(d) from Fig. 7(b). Brenner theory [Eq. (23)] (–), parallel wall Taylor–Aris [Eq. (1)] (..), full Taylor–Aris [Eq. (26a)] (- -), random walk simulations (◇). Here $\mathrm{Pe}_{\mathrm{eff}}^{-1}=D_{\mathrm{eff}}/Q$.

lation of Lagrangian velocities from pore throat to pore throat. The increase in the pore wall fluctuations tends to widen the Lagrangian velocity distribution within pores. For instance, for large fluctuations of the pore walls, particles traveling close to the wall may take a long time to leave the pore, in particular, if they remain trapped inside a recirculation zone. On the other hand, the increase in the pore wall fluctuations increases the convergence of flow lines at pore throats. The latter implies a decorrelation of Lagrangian velocities since it is easier for particles to jump between streamlines by diffusion. The widening of the Lagrangian velocity distribution implies an increase in the asymptotic dispersion coefficient while the decrease in the Lagrangian velocity correlation implies a decrease in the asymptotic dispersion coefficient. Thus, when increasing pore wall fluctuations, the changes in the Lagrangian velocity distribution and in the Lagragian velocity correlation have an antagonist effect on the asymptotic dispersion coefficient. The existence of these two competitive effects implies that pore wall fluctuations can either increase or decrease the asymptotic dispersion coefficient depending on the relative strength of these two effects (Fig. 8).

For small aspect ratio $\epsilon$, i.e., for elongated pores, the dominant effect of the increase in the pore wall fluctuations is a stronger convergence of flow lines at pore throats and thus a decorrelation of the Lagrangian velocities. This implies a decrease in the asymptotic dispersion coefficient. On the other hand, for a larger aspect ratio, the increase of the pore wall fluctuations leads to the existence of recirculation zones (Fig. 2). The trapping of particles in these recirculation zones implies a significant widening of the Lagrangian velocity distribution within a pore. Therefore, in this case, the latter effect is found to dominate over the decorrelation of Lagrangian velocities and the asymptotic dispersion coefficient is increased.

Our Taylor–Aris approximation in essence neglects the effect of the convergence and divergence of streamlines. By neglecting this effect this approximation leads to a stronger correlation of Lagrangian velocities and thus a larger

asymptotic dispersion coefficient than predicted by the full numerical solution (Fig. 11). On the other hand, the Brenner solution includes the effect of the convergence and divergence of flow lines and thus reproduces the numerical simulations satisfactorily.

This is a qualitative interpretation of the presented results. We are currently performing a fully quantitative analysis of the Lagrangian velocity properties within such system using the methods proposed in Refs. 65 and 66).

## IV. SUMMARY AND DISCUSSION

Using an analytical perturbation solution for the flow field, we have studied solute dispersion at asymptotic times in two-dimensional channels with periodic wavy walls. To do this we used the method of local moments.[5] In particular we focused on the effects of varying the amplitude and wavelength of the boundary fluctuations.

First, we employed an approximation analogous to the Taylor–Aris theory[23] [Eq. (26a)]. By making this assumption we analytically calculated the effective dispersion coefficients. We found that for a fixed flow rate, dispersive effects increase monotonically with the amplitude of fluctuation and with decreasing wavelength, i.e., the shorter and wider the pores the larger the dispersive effects. Additionally, under the Taylor–Aris assumption, dispersion effects scale linearly with Peclet number, implying that the behavior while quantitatively different (i.e., at large Peclet numbers dispersive effects dominate diffusion, while at smaller values diffusion still plays a role) is qualitatively similar.

In order to check the validity of these Taylor–Aris-type assumptions we computed the full solution to the local moment equation numerically [Eq. (23)] and found results that differed significantly. First, we found that the qualitative effects on effective dispersion are quite different when varying the Peclet number. We did not find a simple linear scaling that one might expect. The behavior at Pe=10 was qualitatively different from that at Pe=100, which in turn was qualitatively different from that at Pe=1000. For small Reynolds number flows (i.e., $\mathrm{Re}<1$), as studied here, one expects the flow field to look the same regardless of the flow rate since advective effects are negligible on flow. However, while the flow fields at different flow rates, i.e., at different Peclet numbers, look identical, the transport behavior differs significantly.

Second, we found cases where increasing the curvature (i.e., increasing the amplitude of fluctuation or decreasing the wavelength) actually led to a decrease in the effective dispersion. We observed this particularly for the larger Peclet number cases. While this may be surprising, especially given the results of the "Taylor" approximation, such a possibility has previously been predicted heuristically in Ref. 36. We present a tentative explanation for these observation based on a Lagrangian interpretation, which will be pursued in greater detail as future work.

Finally, we also found that while increases in dispersion did occur, particularly for large fluctuations and short wavelengths, these increases were much smaller than those predicted by our Taylor approximation. This suggests that while curvature can influence the effective dispersion, its influence may not be as large as one might expect from a simplified analysis.

In order to validate our analysis we studied the transport of a passive contaminant in such flows using a high accuracy numerical random walk method. We found in all cases that the dispersion coefficient predicted by the full "Brenner" solution [Eq. (23)] compared very well with these simulations, unlike the Taylor–Aris approximation model [Eq. (26a)], which seriously overpredicted dispersion. For most cases, taking the original Taylor–Aris solution [Eq. (1)] for a channel with no fluctuations provided a better estimate than the approximate local moment solution, although it was still off. Our Taylor–Aris approximation consisted of two parts, neglecting horizontal gradients and advection transverse to the mean flow direction. As shown in Ref. 38 this approximation falls apart when $\mathrm{Pe}\,\epsilon^2=O(1)$ and these neglected features appear to play an important role. Additionally the expansion proposed in Eq. (25) may become invalid for some of the larger values of $a$.

In summary, changes in the periodic boundary fluctuations in a channel can lead to both increases and decreases in effective dispersion. This statement may have strong implications for applied fields such as transport through porous/fractured media where curvature in the flow field is commonplace, or in microfluidics where such curvature effects may be exploited to control mixing.

## APPENDIX A: THE FLOW STREAMFUNCTIONS

The zeroth, second, and fourth order flow rates, $Q_0$, $Q_2$, and $Q_4$ are given by

$$Q_0=\left[\frac{(1-4a^2)^{5/2}}{1+2a^2}\right]\bar{Q},$$

$$Q_2=\left[-\frac{12}{5}\frac{(1-4a^2)^{7/2}\pi^2a^2}{(1+2a^2)^2}\right]\bar{Q}, \tag{A1}$$

$$Q_4=\left[\frac{144}{25}\frac{(1-4a^2)^{9/2}\pi^4a^4}{(1+2a^2)^3}-\frac{(1-4a^2)^{5/2}\pi^4}{175(1+2a^2)^2}(7648a^6-7680a^4+2406a^2+214(1-4a^2)^{5/2}-241)\right]\bar{Q}.$$

The zeroth, second, and fourth order contributions to the stream function, given in Ref. 12, are

$$\Psi_0=\frac{Q_0}{4}(3\xi-\xi^3), \tag{A2}$$

$$\Psi_2=\frac{Q_2}{Q_0}\psi_0+\frac{3Q_0}{40}\left[4\left(\frac{dh}{d\eta}\right)^2-h\frac{dh}{d\eta}\right]\xi(\xi^2-1)^2, \tag{A3}$$

$$\Psi_4 = \left[\frac{Q_4}{Q_0} - \left(\frac{Q_2}{Q_0}\right)^2\right]\psi_0 + \frac{Q_2}{Q_0}\psi_2 - \frac{Q_0}{5600}\Bigg[(408 + 1800\xi^2) \times \left(\frac{dh}{d\eta}\right)^4 + (684 - 1800\xi^2)h\left(\frac{dh}{d\eta}\right)^2\frac{d^2h}{d\eta^2} - (270 - 180\xi^2)h^2\left(\frac{d^2h}{d\eta^2}\right)^2 - (248 - 240\xi^2)h^2\frac{dh}{d\eta}\frac{d^3h}{d\eta^3} + (19 - 15\xi^2)h^3\frac{d^4h}{d\eta^4}\Bigg]\xi(\xi^2 - 1)^2, \quad \text{(A4)}$$

where

$$\eta = \epsilon x, \quad \xi = \frac{y}{h(\eta)} \quad \text{and} \quad h(\eta) = \frac{1}{2} + a\sin(2\pi\eta). \quad \text{(A5)}$$

## APPENDIX B: TAYLOR METHOD

Integrating Eq. (24) twice with respect to $y$ gives

$$\chi(\mathbf{x}) = \int dy f(\mathbf{x}) + A(x)y + B(x), \quad \text{(B1)}$$

where $f(\mathbf{x}) = \int dy u'(\mathbf{x})$. The symmetry of the channel geometry implies that $\chi$ is symmetric about $y=0$, which yields $A(x) \equiv 0$. As the average of $\chi$ is zero, we obtain

$$B(x) = -\bar{F}(x), \quad \text{(B2)}$$

where $F(\mathbf{x}) = \int dy f(\mathbf{x})$. Thus, we obtain for $\chi(\mathbf{x})$,

$$\chi(\mathbf{x}) = F(\mathbf{x}) - \bar{F}(x). \quad \text{(B3)}$$

## APPENDIX C: RANDOM WALK SIMULATIONS

The transport problem is solved numerically by random walk simulations based on the Langevin Eq. (31). In discrete time, the equation of motion of the $n$th solute particle reads as

$$x^{(n)}(t + \Delta t|\mathbf{x}') = x(t, \mathbf{x}') + u[\mathbf{x}(t|\mathbf{x}')]\Delta t + \sqrt{2D\Delta t}\,\eta_1,$$
$$y^{(n)}(t + \Delta t|\mathbf{x}') = y(t|\mathbf{x}') + v[\mathbf{x}(t|\mathbf{x}')]\Delta t + \sqrt{2D\Delta t}\,\eta_2. \quad \text{(C1)}$$

The $\eta_i (i = 1, \ldots, d)$ are independently distributed Gaussian random variables with zero mean and variance one. The impermeable channel walls are modeled as reflecting boundaries.

The $i$th local moment is given by summation over the $i$th power of the particle trajectories of all simulated particles originating from $\mathbf{x}'$,

$$\mu^{(i)}(t|\mathbf{x}') = \lim_{N\to\infty}\frac{1}{N}\sum_{n=1}^{\infty}[x_1^{(n)}(t|\mathbf{x}')]^i. \quad \text{(C2)}$$

The global moments are obtained by summation over all initial positions $\mathbf{x}'$, which are distributed according to $\rho(\mathbf{x}')$,

$$m^{(i)}(t) = \lim_{M\to\infty}\frac{1}{M}\sum_{m=1}^{M}\mu^{(i)}(t|\mathbf{x}'^{(m)}). \quad \text{(C3)}$$

The asymptotic effective dispersion coefficient then is given by

$$D^e = \lim_{t\to\infty}\frac{1}{2}\frac{d}{dt}[m^2(t) - m^{(1)}(t)^2]. \quad \text{(C4)}$$

The simulations presented release $N$ particles from each initial position. The line source is represented by $M$ equidistantly positioned point sources along the cross section of the channel at $x=0$.


[1] L. E. Locascio, "Microfluidic mixing," Anal. Bioanal. Chem. **379**, 325 (2004).
[2] A. Tripathi, O. Bozkurt, and A. Chauhan, "Dispersion in microchannels with temporal temperature variations," Phys. Fluids **17**, 103607 (2005).
[3] J. H. Forrester and D. F. Young, "Flow through converging-diverging tube and its implications in occlusive disease," J. Biomech. **3**, 297 (1970).
[4] N. S. Abdullah and D. B. Das, "Modelling nutrient transport in hollow bre membrane bioreactor for growing bone tissue with consideration of multicomponent interactions," Chem. Eng. Sci. **62**, 5821 (2007).
[5] H. Brenner, "Dispersion resulting from flow through spatially periodic porous media," Proc. R. Soc. London, Ser. A **1430**, 81 (1980).
[6] D. L. Koch and J. F. Brady, "A non-local description of advection-diffusion with application to dispersion in porous media," J. Fluid Mech. **180**, 387 (1987).
[7] D. L. Koch and J. F. Brady, "The symmetry properties of the effective diffusivity tensor in anisotropic porous media," Phys. Fluids **30**, 642 (1987).
[8] J. Salles, J.-F. Thovert, R. Delannay, L. Prevors, J.-L. Auriault, and P. M. Adler, "Taylor dispersion in porous media. Determination of the dispersion tensor," Phys. Fluids A **5**, 2348 (1993).
[9] D. A. Edwards, M. Shapiro, H. Brenner, and M. Shapira, "Dispersion of inert solutes in spatially periodic, two-dimensional model porous media," Transp. Porous Media **6**, 337 (1991).
[10] G. Dagan and A. Fiori, "The influence of pore-scale dispersion on concentration statistical moments in transport through heterogeneous aquifers," Water Resour. Res. **33**, 1595, DOI: 10.1029/97WR00803 (1997).
[11] A. Fiori, "On the influence of pore-scale dispersion in nonergodic transport in heterogeneous formations," Transp. Porous Media **30**, 57 (1998).
[12] P. K. Kitanidis and B. B. Dykaar, "Stokes flow in a slowly varying two-dimensional periodic pore," Transp. Porous Media **26**, 89 (1997).
[13] M. Dentz and J. Carrera, "Mixing and spreading in stratified flow," Phys. Fluids **19**, 017107 (2007).
[14] J. Bear, *Dynamics of Fluids in Porous Media* (Elsevier, New York, 1972).
[15] D. Grubert, "Effective dispersivities for a two-dimensional periodic fracture network by a continuous time random walk analysis of single-intersection simulations," Water Resour. Res. **37**, 41, DOI: 10.1029/2000WR900240 (2001).
[16] J.-R. de Dreuzy, P. Davy, and O. Bour, "Hydraulic properties of two-dimensional random fracture networks following a power law length distribution 1. Effective connectivity," Water Resour. Res. **37**, 2065, DOI: 10.1029/2001WR900011 (2001).
[17] A. M. Tartakovsky, G. Redden, P. C. Lichtner, T. D. Scheibe, and P. Meakin, "Mixing-induced precipitation: Experimental study and multiscale numerical analysis," Water Resour. Res. **44**, W06S04, DOI: 10.1029/2006WR005725 (2008).
[18] P. K. Kitanidis, "Prediction by the method of moments of transport in heterogeneous formations," J. Hydrol. **102**, 453 (1988).
[19] P. K. Kitanidis, "The concept of the dilution index," Water Resour. Res. **30**, 2011, DOI: 10.1029/94WR00762 (1994).
[20] V. Zavala-Sanchez, M. Dentz, and X. Sanchez-Vila, "Characterization of mixing and spreading in a bounded stratified medium," Adv. Water Resour. **32**, 635 (2009).
[21] W. N. Gill and R. Sankarasubramanian, "Exact analysis of unsteady convective diffusion," Proc. R. Soc. London, Ser. A **316**, 341 (1970).

[22]M. Latini and A. J. Bernoff, "Transient anomalous diffusion in Poiseuille flow," J. Fluid Mech. **441**, 339 (2001).
[23]G. I. Taylor, "Dispersion of soluble matter in solvent flowing slowly through a tube," Proc. R. Soc. London, Ser. A **223**, 446 (1954).
[24]R. Mauri, "Lagrangian self diffusion of Brownian particles in periodic flow fields," Phys. Fluids **7**, 275 (1995).
[25]R. Aris, "On the dispersion of a solute in a fluid flowing through a tube," Proc. R. Soc. London, Ser. A **235**, 67 (1956).
[26]S. R. Brown, H. W. Stockman, and S. J. Reeves, "Applicability or the Reynolds equation for modelling fluid flow between rough surfaces," Geophys. Res. Lett. **22**, 2537, DOI: 10.1029/95GL02666 (1995).
[27]V. V. Mourenzo, J. F. Thovert, and P. Adler, "Permeability of a single fracture: Validity of Reynolds equation," J. Phys. II **5**, 465 (1995).
[28]M. J. Nicholl, H. Rajaram, R. J. Glass, and R. Detwiler, "Saturated flow in a single fracture: evaluation of the Reynolds equation in measured aperture fields," Water Resour. Res. **35**, 3361, DOI: 10.1029/1999WR900241 (1999).
[29]D. M. Tartakovsky and D. Xiu, "Stochastic analysis of transport in tubes with rough walls," J. Comput. Phys. **217**, 248 (2006).
[30]D. Xiu and D. M. Tartakovsky, "Numerical methods for differential equations in random domains," SIAM J. Sci. Comput. (USA) **28**, 1167 (2006).
[31]L. W. Gelhar, *Stochastic Subsurface Hydrology* (Prentice-Hill, Englewood Cliffs, 1993).
[32]G. Drazer, H. Auradou, J. Koplik, and J. P. Hulin, "Self-affine front in self-affine fractures: Large and small-scale structure," Phys. Rev. Lett. **92**, 014501 (2004).
[33]G. Drazer and J. Koplik, "Transport in rough self-affine fractures," Phys. Rev. E **66**, 026303 (2002).
[34]R. Smith, "Longitudinal dispersion coefficients for varying channels," J. Fluid Mech. **130**, 299 (1983).
[35]G. N. Mercer and A. J. Roberts, "A centre manifold description of contaminant dispersion in channels with varying flow properties," SIAM J. Appl. Math. **50**, 1547 (1990).
[36]S. Rosencrans, "Taylor dispersion in curved channels," SIAM J. Appl. Math. **57**, 1216 (1997).
[37]R. K. Prud'Homme and D. A. Hoagland, "Taylor-Aris dispersion arising from flow in a sinusoidal tube," AIChE J. **31**, 236 (1999).
[38]E. Yariv and K. D. Dorfman, "Electrophoretic transport through channels of periodically varying cross section," Phys. Fluids **19**, 037101 (2007).
[39]N. Laachi, M. Kenward, E. Yariv, and K. D. Dorfman, "Force-driven transport through periodic entropy barriers," Eur. Phys. Lett. **80**, 50009 (2007).
[40]P. S. Burada, G. Schmid, D. Reguera, J. M. Rubi, and P. Hanggi, "Biased diffusion in confined media: Test of the Fick-Jacons approximation and validity criteria," Phys. Rev. E **75**, 051111 (2007).
[41]J. P. Bouchaud and A. Georges, "Anomalous diffusion in disordered media: Statistical mechanisms, models and physical applications," Phys. Rep. **195**, 127 (1990).
[42]M. B. Isichenko, "Percolation, stochastic topography, and transport in random media," Rev. Mod. Phys. **64**, 961 (1992).
[43]S. W. Jones and W. R. Young, "Shear dispersion and anomalous diffusion by chaotic advection," J. Fluid Mech. **280**, 149 (1994).
[44]R. Haggerty and S. M. Gorelick, "Multiple-rate mass transfer for modeling diffusion and surface reactions in media with pore-scale heterogeneity," Water Resour. Res. **310**, 2383 (1995).
[45]J. Carrera, X. Sánchez-Vila, I. Benet, A. Medina, G. Galarza, and J. Guimerà, "On matrix diffusion: Formulations, solution methods, and qualitative effects," Hydrogeol. J. **6**, 178 (1998).
[46]S. Sisavath, X. Jing, and R. W. Zimmerman, "Creeping flow through a pipe of varying radius," Phys. Fluids **13**, 2762 (2001).
[47]J. Cao and P. K. Kitanidis, "Adaptive finite element simulation of Stokes flow in porous media," Adv. Water Resour. **22**, 17 (1998).
[48]S. Sisavath, A. Al-Yaarubi, C. C. Pain, and R. W. Zimmerman, "A simple mode for deviation from the cubic law for a fracture undergoing dilation or closure," Pure Appl. Geophys. **160**, 1009 (2003).
[49]H. Brenner and P. M. Adler, "Dispersion resulting from flow through spatially periodic porous media II. Surface and intraparticle transport," Proc. R. Soc. London, Ser. A **1498**, 149 (1982).
[50]I. Frankel and H. Brenner, "On the foundations of generalized Taylor dispersion theory," J. Fluid Mech. **97**, 204 (1989).
[51]M. Shapiro and H. Brenner, "Chemically reactive generalized Taylor dispersion phenomena," AIChE J. **33**, 1155 (1987).
[52]M. Shapiro and H. Brenner, "Dispersion of a chemically reactive solute in a spatially periodic model of a porous medium," Chem. Eng. Sci. **43**, 551 (1988).
[53]B. B. Dykaar and P. K. Kitanidis, "Macrotransport of biologically reactive solute through porous media," Water Resour. Res. **32**, 307, DOI: 10.1029/95WR03241 (1996).
[54]C. Pozrikidis, "Creeping flow in two-dimensional channels," J. Fluid Mech. **180**, 495 (1987).
[55]P. K. Kundu, *Fluid Mechanics* (Academic, San Diego, 1990).
[56]P. A. Witherspoon, J. S. Y. Wang, K. Iwai, and J. E. Gale, "Validity of the cubic law for fluid flow in a deformable rock fracture," Water Resour. Res. **16**, 1016, DOI: 10.1029/WR016i006p01016 (1980).
[57]R. Detwiler, H. Rajaram, and R.J. Glass, "Solute transport in variable-aperture fractures: An investigation of the relative importance of Taylor dispersion and macrodispersion," Water Resour. Res. **36**, 1611, DOI: 10.1029/2000WR900036 (2000).
[58]G. K. Batchelor, *An Introduction to Fluid Mechanics* (Cambridge University Press, Cambridge, 1976).
[59]W. Kinzelbach, "The random-walk method in pollutant transport simulation," *Groundwater Flow and Quality Modeling*, NATO Advanced Studies Institute, Series C (Reidel, Dordrecht, 1988), pp. 227–246.
[60]A. Tompson and L. Gelhar, "Numerical simulation of solute transport in three-dimensional, randomly heterogeneous porous media," Water Resour. Res. **260**, 2541 (1990).
[61]U. Jaekel and H. Vereecken, "Renormalization group analysis of macrodispersion in a directed random flow," Water Resour. Res. **33**, 2287, DOI: 10.1029/97WR00553 (1997).
[62]M. Dentz, H. Kinzelbach, S. Attinger, and W. Kinzelbach, "Numerical studies of the transport behavior of a passive solute in a two-dimensional incompressible random flow field," Phys. Rev. E **67**, 046306 (2003).
[63]M. Dentz, H. Kinzelbach, S. Attinger, and W. Kinzelbach, "Temporal behavior of a solute cloud in a heterogeneous porous medium 3. Numerical simulations," Water Resour. Res. **38**, 1118, DOI: 10.1029/2001WR000436 (2002).
[64]H. Risken, *The Fokker-Plank Equation* (Springer, New York, 1996).
[65]T. LeBorgne, M. Dentz, and J. Carrera, "Lagrangian statistical model for transport in highly heterogeneous velocity fields," Phys. Rev. Lett. **101**, 090601 (2008).
[66]T. LeBorgne, M. Dentz, and J. Carrera, "Spatial Markov processes for modeling Lagrangian particle dynamics in heterogeneous porous media," Phys. Rev. E **78**, 026308 (2008).